DESIGN OF OPTIMAL QUINCUNX FILTER BANKS FOR IMAGE CODING VIA SEQUENTIAL QUADRATIC PROGRAMMING

Yi Chen, Michael D. Adams, and Wu-Sheng Lu

Dept. of Elec. and Comp. Eng., University of Victoria, Victoria, BC, Canada

ABSTRACT

Sequential quadratic programming is used to design high-performance quincunx filter banks for image coding, where the resulting filter banks have perfect reconstruction, linear phase, high coding gain, good frequency selectivity, and certain prescribed vanishing-moment properties. Design examples are presented and compared to various previously proposed filter banks. The new filter banks are shown to be highly effective for image coding, outperforming previously proposed quincunx filter banks in most cases, and outperforming the well-known 9/7 filter bank in some limited cases.

Index Terms— Multidimensional signal processing, optimization methods, wavelet transforms, image coding

1. INTRODUCTION

Quincunx filter banks are two-dimensional (2D) two-channel nonseparable filter banks, and have been shown to be a highly effective tool for image coding applications. In such applications, it is usually desirable for the filter banks to have perfect reconstruction (PR), linear phase, high coding gain, good frequency selectivity, and certain vanishing-moment properties. In the nonseparable case, however, it is very difficult to design filter banks with all of these properties. Most of the existing design techniques employ a transformation of variables [1]. Using these transformation-based methods, one cannot explicitly control the 2D filter frequency responses. In this paper, we show how one can design quincunx filter banks to have all of the aforementioned properties via the lifting framework [2] and sequential quadratic programming (SQP) [3]. Although designs based on the lifting framework have been proposed in [4, 5], these methods only consider interpolating filter banks (i.e., filter banks with two lifting steps). In this paper, we examine the more general case.

The remainder of this paper is structured as follows. Section 2 briefly comments on some notational conventions used herein. Section 3 introduces quincunx filter banks and the aforementioned desirable properties for such filter banks. Section 4 explains the design problem formulation. Design examples are presented in Section 5 and their effectiveness for image coding is demonstrated in Section 6. Finally, Section 7 concludes with a summary of our work and some closing remarks.

2. NOTATION AND TERMINOLOGY

In this paper, the sets of integers, even integers, and real numbers are denoted as $\mathbb{Z}$, $\mathbb{Z}_e$ and $\mathbb{R}$, respectively. Matrices and vectors are denoted by upper and lower case boldface letters, respectively. For matrix multiplication, we define the product notation as $\prod_{k=M}^{N} \boldsymbol{A}_k \triangleq \boldsymbol{A}_N \boldsymbol{A}_{N-1} \cdots \boldsymbol{A}_{M+1} \boldsymbol{A}_M$ for $N \geq M$. For convenience, a polynomial function of the elements of a vector $\boldsymbol{x}$ is simply referred to as a polynomial function of $\boldsymbol{x}$. Let $\boldsymbol{n} = [n_0 \;\; n_1]^T$ and $\boldsymbol{z} = [z_0 \;\; z_1]^T$. Then, we define $|\boldsymbol{n}| = n_0 + n_1$ and $\boldsymbol{z}^{\boldsymbol{n}} = z_0^{n_0} z_1^{n_1}$. Furthermore, for a matrix $\boldsymbol{M} = [\boldsymbol{m}_0 \;\; \boldsymbol{m}_1]$ with $\boldsymbol{m}_k$ being the kth column of $\boldsymbol{M}$, we define $\boldsymbol{z}^{\boldsymbol{M}} = [\boldsymbol{z}^{\boldsymbol{m}_0} \;\; \boldsymbol{z}^{\boldsymbol{m}_1}]^T$. In what follows, we will use $\boldsymbol{M}$ to denote the generating matrix $\left[\begin{smallmatrix} 1 & 1 \\ 1 & -1 \end{smallmatrix}\right]$ of the quincunx lattice.

The Fourier transform of a sequence h is denoted as $\hat{h}$. A 2D filter H with impulse response h is said to be linear phase with group delay $\boldsymbol{c}$ if, for some $\boldsymbol{c} \in \frac{1}{2}\mathbb{Z}^2$, $h[\boldsymbol{n}] = h[2\boldsymbol{c} - \boldsymbol{n}]$ for all $\boldsymbol{n} \in \mathbb{Z}^2$. For the linear-phase filter H, its frequency response $\hat{h}(\boldsymbol{\omega})$ can be expressed as $\hat{h}(\boldsymbol{\omega}) = e^{-j\boldsymbol{\omega}^T \boldsymbol{c}} \hat{h}_a(\boldsymbol{\omega})$, where $\hat{h}_a(\boldsymbol{\omega}) = \sum_{\boldsymbol{n} \in \mathbb{Z}^2} h[\boldsymbol{n}] \cos\left[\boldsymbol{\omega}^T (\boldsymbol{n} - \boldsymbol{c})\right]$. For convenience, we call $\hat{h}_a(\boldsymbol{\omega})$ the signed amplitude response of H. For two images x and x_r of size $N_0 \times N_1$ with P bits per sample, we define the peak-signal-to-noise ratio (PSNR) as PSNR $= 20\log_{10}\left(\frac{2^P - 1}{\sqrt{\text{MSE}}}\right)$, where MSE $= \frac{1}{N_0 N_1} \sum_{\boldsymbol{n}} \left(x_r[\boldsymbol{n}] - x[\boldsymbol{n}]\right)^2$.

3. QUINCUNX FILTER BANKS

Fig. 1 shows the canonical form of a quincunx filter bank, which consists of analysis filters H_0 and H_1, synthesis filters G_0 and G_1, and $\boldsymbol{M}$-fold downsamplers and upsamplers. In wavelet-based image coding, the filter bank is applied recursively to the lowpass channel, resulting in an octave-band filter bank. For an L-level octave-band filter bank, the equivalent nonuniform filter bank has $L+1$ channels with analysis filters $\{\text{H}_i'\}$ and synthesis filters $\{\text{G}_i'\}$. The analysis filter transfer functions $\{H_i'(\boldsymbol{z})\}$ are given by

$$H_i'(\boldsymbol{z}) = \begin{cases} \prod_{k=0}^{L-1} H_0\left(\boldsymbol{z}^{\boldsymbol{M}^k}\right) & i = 0 \\ H_1\left(\boldsymbol{z}^{\boldsymbol{M}^{L-i}}\right) \prod_{k=0}^{N-i-1} H_0\left(\boldsymbol{z}^{\boldsymbol{M}^k}\right) & 1 \leq i \leq L-1 \\ H_1(\boldsymbol{z}) & i = L, \end{cases}$$

and the synthesis filter transfer functions $\{G_i'(\boldsymbol{z})\}$ can be similarly derived [6]. Next, we consider the relationships between quincunx filter banks and the desirable properties identified in Section 1.

In image coding, it is often desirable for the filter banks to have PR to facilitate the construction of a lossless compression system, and linear phase to avoid phase distortion. Here, we introduce a lifting-based parameterization of quincunx filter banks such that the PR and linear-phase conditions are automatically satisfied. Fig. 2 shows the structure of the lifting realization of a quincunx filter bank. Essentially, the filter bank is realized in its polyphase form, and the analysis and synthesis filtering are each performed by a ladder network of 2λ lifting filters $\{\text{A}_k\}$. Due to the use of the lifting framework, the PR condition is automatically satisfied. Given the lifting filters $\{\text{A}_k\}$, the corresponding analysis filter transfer functions $H_0(\boldsymbol{z})$ and $H_1(\boldsymbol{z})$ can be calculated as $H_k(\boldsymbol{z}) = H_{k,0}\left(\boldsymbol{z}^{\boldsymbol{M}}\right) + z_0 H_{k,1}\left(\boldsymbol{z}^{\boldsymbol{M}}\right)$, where

$$\begin{bmatrix} H_{0,0}(\boldsymbol{z}) & H_{0,1}(\boldsymbol{z}) \\ H_{1,0}(\boldsymbol{z}) & H_{1,1}(\boldsymbol{z}) \end{bmatrix} = \prod_{k=1}^{\lambda} \left(\begin{bmatrix} 1 & A_{2k}(\boldsymbol{z}) \\ 0 & 1 \end{bmatrix} \begin{bmatrix} 1 & 0 \\ A_{2k-1}(\boldsymbol{z}) & 1 \end{bmatrix} \right).$$

This work was supported, in part, by the Natural Sciences and Engineering Research Council of Canada.

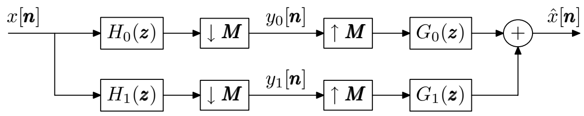

Fig. 1. Quincunx filter bank (canonical form).

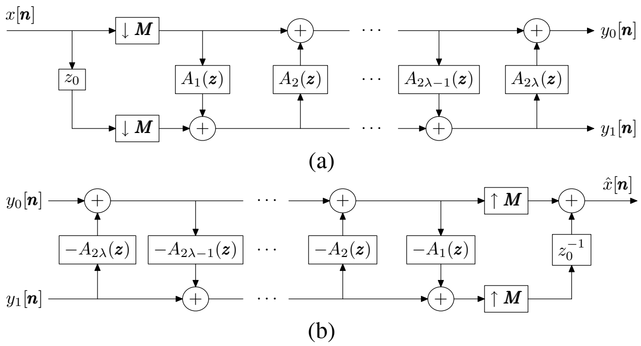

Fig. 2. Lifting realization of a quincunx filter bank. (a) Analysis side and (b) synthesis side.

The synthesis filter transfer functions $G_0(z)$ and $G_1(z)$ can then be trivially computed as $G_k(\boldsymbol{z}) = (-1)^{1-k} z_0^{-1} H_{1-k}(-\boldsymbol{z})$.

With the lifting framework, the linear-phase property can also be easily imposed if each of the lifting filters A_k has linear phase with group delay $\boldsymbol{c}_k$ satisfying $\boldsymbol{c}_k = (-1)^k \left[\frac{1}{2} \;\; \frac{1}{2}\right]^T$. With this choice of lifting filters, the analysis filters H_0 and H_1 have linear phase with group delays $\boldsymbol{d}_0 = [0 \;\; 0]^T$ and $\boldsymbol{d}_1 = [-1 \;\; 0]^T$, respectively.

Let $\boldsymbol{x}$ denote a vector containing all independent coefficients of the 2λ lifting filters. Next, we examine the relationships between $\boldsymbol{x}$ and the filter bank properties of interest (i.e., coding gain, frequency selectivity, and vanishing moment properties), beginning with the coding gain.

Coding gain is a measure of the energy compaction ability of a filter bank. For an L-level octave-band quincunx filter bank, the coding gain G_{SBC} [7] is computed as

$$G_{SBC} = \prod_{k=0}^{L} (A_k B_k / \alpha_k)^{-\alpha_k},$$

where $A_k = \sum_{\boldsymbol{m} \in \mathbb{Z}^2} \sum_{\boldsymbol{n} \in \mathbb{Z}^2} h'_k[\boldsymbol{m}] h'_k[\boldsymbol{n}] r[\boldsymbol{m} - \boldsymbol{n}]$, $B_k = \alpha_k \sum_{\boldsymbol{n} \in \mathbb{Z}^2} g'^2_k[\boldsymbol{n}]$, $\alpha_0 = 2^{-L}$, $\alpha_k = 2^{-(L+1-k)}$ for $k = 1, 2, \ldots, L$, $h'_k[\boldsymbol{n}]$ and $g'_k[\boldsymbol{n}]$ are the impulse responses of the equivalent analysis and synthesis filters H'_k and G'_k, respectively, and r is the normalized autocorrelation of the input. Depending on the source image model, r is given by

$$r[n_0, n_1] = \begin{cases} \rho^{|n_0| + |n_1|} & \text{for separable model} \\ \rho^{\sqrt{n_0^2 + n_1^2}} & \text{for isotropic model,} \end{cases}$$

where ρ is the correlation coefficient (typically, $0.90 \leq \rho \leq 0.95$). The coding gain is a nonlinear function of $\boldsymbol{x}$.

In filter bank design problems, we also desire good frequency selectivity to minimize aliasing between subbands. To quantify the frequency selectivity, we define a frequency response error function to measure the difference between the actual and desired frequency responses. For a linear-phase filter H_k, the error function e_{h_k} is defined as

$$e_{h_k} = \int_{[-\pi,\, \pi)^2} W(\boldsymbol{\omega}) \left| \hat{h}_{a_k}(\boldsymbol{\omega}) - D \hat{h}_{d_k}(\boldsymbol{\omega}) \right|^2 \mathrm{d}\boldsymbol{\omega},$$

where $\hat{h}_{a_k}(\boldsymbol{\omega})$ is the signed amplitude response of H_k as defined earlier in Section 2, $\hat{h}_{d_k}(\boldsymbol{\omega})$ is the desired frequency response with a diamond-shaped passband/stopband, D is a scaling factor, and $W(\boldsymbol{\omega})$ is a weighting function used to control the relative importance of the passband and stopband. In order for the filter H_k to have good frequency selectivity, the error function is required to satisfy $e_{h_k} \leq \delta_{h_k}$, where δ_{h_k} is a prescribed upper bound on the error. The constraints on the frequency selectivity of the analysis filters H_0 and H_1 are polynomial inequalities in $\boldsymbol{x}$.

Now we consider the relationship between the lifting-filter coefficients and vanishing moments. The presence of vanishing moments is important as it helps to reduce the number of nonzero coefficients in the higher-frequency subbands, and improve the visual quality of the reconstructed images for lossy compression. For quincunx filter banks, to have N primal and $\tilde{N}$ dual vanishing moments, the lowpass and highpass analysis filters H_0 and H_1 should have Nth- and $\tilde{N}$th-order zeros at $[\pi \;\; \pi]^T$ and $[0 \;\; 0]^T$, respectively. Recall that, due to the lifting parameterization employed, H_0 and H_1 are linear phase with group delays $\boldsymbol{d}_0$ and $\boldsymbol{d}_1$, respectively. Therefore, to have N primal vanishing moments, the lowpass analysis filter coefficients $h_0[\boldsymbol{n}]$ should satisfy $\sum_{\boldsymbol{n} \in \mathbb{Z}^2} (-1)^{|\boldsymbol{n} - \boldsymbol{d}_0|} h_0[\boldsymbol{n}] \, (\boldsymbol{n} - \boldsymbol{d}_0)^{\boldsymbol{m}} = 0$ for all $|\boldsymbol{m}| \in \mathbb{Z}_e$ and $|\boldsymbol{m}| < N$. Similarly, to have $\tilde{N}$ dual vanishing moments, the highpass analysis filter coefficients $h_1[\boldsymbol{n}]$ should satisfy $\sum_{\boldsymbol{n} \in \mathbb{Z}^2} h_1[\boldsymbol{n}] \, (\boldsymbol{n} - \boldsymbol{d}_1)^{\boldsymbol{m}} = 0$ for all $|\boldsymbol{m}| \in \mathbb{Z}_e$ and $|\boldsymbol{m}| < \tilde{N}$. Thus, the conditions on vanishing moments are polynomial equations in $\boldsymbol{x}$. Moreover, for filter banks with two lifting filters A_1 and A_2, if $\tilde{N} \geq N$, the conditions can be expressed as a set of linear equations in the lifting-filter coefficients [5].

4. DESIGN PROBLEM FORMULATION

In our design problem, we use the lifting parameterization to satisfy the PR and linear-phase conditions. Then, we maximize the coding gain subject to constraints on frequency selectivity and vanishing moments. The design problem is solved by SQP [3].

SQP is an effective tool for solving general nonlinear constrained optimization problems of the form

$$\begin{array}{lll} \text{minimize} & f(\boldsymbol{x}) & \\ \text{subject to:} & a_i(\boldsymbol{x}) = 0 & \text{for } i = 1, 2, \ldots, p, \text{ and/or} \\ & c_k(\boldsymbol{x}) \geq 0 & \text{for } k = 1, 2, \ldots, q, \end{array}$$

where $f(\boldsymbol{x})$, $a_i(\boldsymbol{x})$, and $c_k(\boldsymbol{x})$ are continuous functions, whose first- and second-order partial derivatives exist and are continuous. The SQP method solves the constrained problem by iteratively solving quadratic programming (QP) subproblems in a sequential manner. The QP subproblems can be solved efficiently using a number of software packages, such as the MATLAB optimization toolbox and the SeDuMi [8] package.

We begin with the design of filter banks having two lifting steps. As mentioned earlier, in this case, the vanishing moment conditions can be expressed as a linear system of equations in the lifting-filter coefficient vector $\boldsymbol{x}$ given by

$$\boldsymbol{A}\boldsymbol{x} = \boldsymbol{b}, \tag{1}$$

where $\boldsymbol{x} \in \mathbb{R}^{n \times 1}$, $\boldsymbol{A} \in \mathbb{R}^{m \times n}$ with rank r, $\boldsymbol{b} \in \mathbb{R}^{m \times 1}$ and $m < n$. By computing the singular value decomposition (SVD) of $\boldsymbol{A} = \boldsymbol{U}\boldsymbol{S}\boldsymbol{V}^T$, the solutions to (1) can be parameterized as $\boldsymbol{x} = \boldsymbol{A}^{+}\boldsymbol{b} + \boldsymbol{V}_r \boldsymbol{\phi}$, where $\boldsymbol{A}^{+}$ is the Moore-Penrose pseudoinverse of $\boldsymbol{A}$, $\boldsymbol{V}_r$ is a matrix composed of the last $n - r$ columns of $\boldsymbol{V}$, and $\boldsymbol{\phi}$ is an arbitrary vector with $n - r$ elements. In what follows, we will use $\boldsymbol{\phi}$ as the design vector. In this way, the number of free variables is reduced from n to $n-r$ and the vanishing moment conditions are automatically satisfied for any choice of $\boldsymbol{\phi}$. The coding gain function G_{SBC}, and frequency response error functions e_{h_0} and e_{h_1} can each be expressed as a function of $\boldsymbol{\phi}$. Therefore, the design problem becomes

$$\begin{array}{ll} \text{minimize} & -\log_{10}\left[G_{SBC}(\boldsymbol{\phi})\right] \\ \text{subject to:} & \delta_{h_k}(\boldsymbol{\phi}) - e_{h_k}(\boldsymbol{\phi}) \geq 0 \quad \text{for } k=0,1. \end{array} \tag{2}$$

The solution to (2) then leads to a filter bank with PR, linear phase, high coding gain, good frequency selectivity, and certain prescribed vanishing moment properties.

For filter banks with more than two lifting steps, the vanishing moment conditions are no longer linear. We write the conditions as

$$a_i(\boldsymbol{x}) = 0 \quad \text{for} \quad i = 1,2,\ldots,\lceil\tilde{N}/2\rceil^2 + \lceil N/2\rceil^2, \tag{3}$$

where $a_i(\boldsymbol{x})$ is a polynomial in $\boldsymbol{x}$. In this case, the design problem has equality constraints on vanishing moments and inequality constraints on frequency selectivity, and can be written as

$$\begin{array}{ll} \text{minimize} & -\log_{10}\left[G_{SBC}(\boldsymbol{x})\right] \\ \text{subject to:} & a_i(\boldsymbol{x}) = 0 \quad \text{for } i = 1,2,\ldots,\lceil\tilde{N}/2\rceil^2 + \lceil N/2\rceil^2, \\ & \delta_{h_k}(\boldsymbol{x}) - e_{h_k}(\boldsymbol{x}) \geq 0 \quad \text{for } k=0,1. \end{array} \tag{4}$$

The equality constraints in (3) are only approximately satisfied. That is, the moments associated with the desired vanishing moment conditions are small but not necessarily zero. To further reduce the moments in question, we can apply an adjustment step after obtaining the solution $\boldsymbol{x}^*$ to (4). This step is formulated as follows. When $\|\boldsymbol{\delta_x}\|$ is small, the linear approximation of $a_i(\boldsymbol{x}^* + \boldsymbol{\delta_x})$ is obtained by $a_i(\boldsymbol{x}^* + \boldsymbol{\delta_x}) = a_i(\boldsymbol{x}^*) + \boldsymbol{g}_i^T\boldsymbol{\delta_x}$, where $\boldsymbol{g}_i$ is the gradient of a_i at the point $\boldsymbol{x}^*$. This adjustment process can then be formulated as the following optimization problem:

$$\begin{array}{ll} \text{minimize} & \sum_{i=1,2,\ldots,\lceil\tilde{N}/2\rceil^2+\lceil N/2\rceil^2}\left[a_i(\boldsymbol{x}^*) + \boldsymbol{g}_i^T\boldsymbol{\delta_x}\right]^2 \\ \text{subject to:} & \|\boldsymbol{\delta_x}\| \leq \beta, \end{array} \tag{5}$$

where β is a prescribed small value. The problem in (5) is equivalent to a second-order cone programming (SOCP) problem, which can be solved efficiently using SeDuMi [8]. Having obtained such a $\boldsymbol{\delta_x}$, we then update the solution to $\boldsymbol{x}^* + \boldsymbol{\delta_x}$. After this adjustment step, the moments in question are typically very close to zero, as will be illustrated by the design example (i.e., SQP2) in the next section.

5. DESIGN EXAMPLES

To demonstrate the effectiveness of the SQP-based design method, we now present two design examples. In the case of both designs, the optimization is carried out for maximal coding gain, assuming a six-level wavelet decomposition and an isotropic image model with correlation coefficient $\rho = 0.95$. Our first design, which will be henceforth referred to as SQP1, employs two lifting steps, each having a diamond support of 6×6. Our second design, henceforth referred to as SQP2, employs three lifting steps, each having a diamond support of 4×4. For comparison purposes, we consider four filter banks designed by previously-proposed methods. The first three of these filter banks, referred to as KS, G62, and OPT1 in what follows, are quincunx filter banks, while the fourth is the well-known separable 9/7 filter bank from the JPEG-2000 standard. The KS filter bank is constructed using the technique of [5], the G62 filter bank is the so

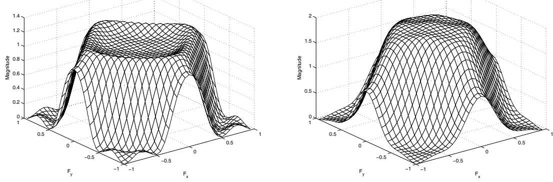

(a) (b)

Fig. 3. Frequency responses of the lowpass (a) analysis and (b) synthesis filters for the SQP1 filter bank.

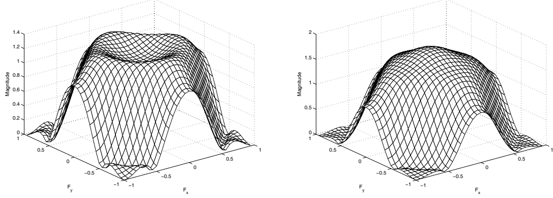

(a) (b)

Fig. 4. Frequency responses of the lowpass (a) analysis and (b) synthesis filters for the SQP2 filter bank.

called $(6,2)$ filter bank proposed in [4], and the OPT1 filter bank is one of the best filter banks designed using the SOCP-based algorithms proposed in [6].

The coding gains and other important characteristics of the above filter banks are shown in Table 1. Obviously, the optimal designs, SQP1 and SQP2, have higher isotropic coding gains than the KS and G62 filter banks. Furthermore, the SQP2 design also has a higher coding gain than the 9/7 filter bank. For SQP2, although the moments in question are not exactly vanishing, they are on the order of 10^{-9} to 10^{-17}, which is small enough to be considered as zero for all practical purposes. The frequency responses of the lowpass filters for SQP1 and SQP2 are shown in Figs. 3 and 4, respectively. We see that these lowpass filters have good diamond-shaped passbands.

In [6], we proposed a SOCP-based method to design quincunx filter banks for image coding. Although the SQP-based method proposed herein and the SOCP-based method in [6] both work by iteratively solving subproblems, they treat the overall design problem in very different ways. Next, we give two examples that compare the performance of these two design methods.

In our first example, we design filter banks which employ two 4×4 lifting filters for maximal coding gain assuming an isotropic model and three levels of decomposition. We apply the SQP- and SOCP-based methods with 625 different initial points. From the 625

Table 1. Comparison of filter bank characteristics.

Name	Support of lifting filters†	Support of analysis filters	G_{SBC} (dB)	$\tilde{N}/N$
SQP1	6×6, 6×6	13×13, 7×7	12.06	2 / 2
SQP2	4×4, 4×4, 4×4	9×9, 13×13	12.23	2 / 2
OPT1	6×6, 6×6	13×13, 7×7	12.06	2 / 2
KS	6×6, 6×6	13×13, 7×7	11.95	6 / 6
G62	6×6, 2×2	13×13, 11×11	11.64	6 / 2
9/7	2, 2, 2, 2	9, 7	12.09	4 / 4

†Support regions are diamond-shaped except for G62 and 9/7.

Table 2. Comparison of SQP- and SOCP-based methods.

	Case 1: two 4×4		Case 2: two 6×6	
	SQP	SOCP	SQP	SOCP
Number of iterations	12.4	24.8	14.5	51.9
Execution time (s)	58.4	77.9	252.8	517.6
G_{SBC} (dB)	11.12	11.12	11.15	11.15

Table 3. Percentage of cases where the SQP1 and SQP2 optimal designs outperform the KS, G62, and OPT1 (quincunx) filter banks.

Filter banks	KS	G62	OPT1
SQP1	80%	95%	56%
SQP2	78%	96%	71%

optimization results, the SQP-based method converges with fewer iterations than the SOCP-based one in 95.7% of the cases, and the total execution time of the SQP-based method is less than that of the SOCP-based one in 85.0% of the cases. The difference between the two methods becomes more obvious for the design of filter banks with two 6×6 lifting filters. In this case, we use 729 different initial points. The SQP-based method converges faster than the SOCP-based one in 96.8% of the cases, requiring fewer iterations than the SOCP-based approach in 727 out of the 729 cases. Table 2 shows the average values of the total number of iterations, overall execution time, and three levels of isotropic coding gains using each of the two methods. Clearly, the coding gains of the optimal solutions obtained by these two methods are essentially the same, while the SQP-based method converges faster than the SOCP-based one in general.

Generally speaking, for a given lifting configuration, the SQP- and SOCP-based methods achieve similar optimal solutions. The SQP-based method usually converges with fewer iterations than the SOCP one. Although the SQP-based method requires more computation in each iteration, when assuming a small number of decomposition levels (e.g., three or four), the overall execution time of the SQP-based method is usually less than that of the SOCP-based method.

6. IMAGE CODING RESULTS

To further demonstrate the effectiveness of our new filter banks, they were employed in the embedded lossy/lossless image codec of [6]. For test data, 27 grayscale images from the JPEG-2000 test set were used. These images were coded in a lossy manner at four compression ratios and then decoded. The difference between the reconstructed images and original images were measured in terms of PSNR. Six and three levels of decomposition were employed in the cases of the quincunx and separable filter banks, respectively.

Table 3 shows the percentage of cases where the SQP1 and SQP2 optimal designs outperform the KS, G62, and OPT1 filter banks, which summarizes all of the lossy compression results for the 27 test images at four compression ratios. We see that our new filter banks SQP1 and SQP2 outperform KS and G62 in about 80% and 95% of the cases, respectively. Furthermore, they also provide slightly better performance than the OPT1 filter bank.

Table 4 shows some typical lossy compression results for an isotropic image, namely for the `finger` (i.e., fingerprint) image. Clearly, the optimal designs SQP1 and SQP2 perform very well, consistently outperforming the KS and G62 quincunx filter banks in all cases, and outperforming OPT1 in most cases. Moreover, our designs achieve better results than the 9/7 filter bank in most cases.

Table 4. Lossy compression results for the `finger` image.

CR†	PSNR (dB)					
	SQP1	SQP2	OPT1	KS	G62	9/7
128	19.88	**19.98**	19.88	19.67	19.19	**19.98**
64	21.72	**21.75**	21.70	21.52	21.18	21.72
32	**24.55**	24.40	24.52	24.36	23.98	24.20
16	27.78	**27.85**	27.75	27.65	27.30	27.61

†compression ratio

This is quite an encouraging result, as the 9/7 filter bank is generally held to be one of the very best in the literature.

7. CONCLUSIONS

In this paper, we showed how one can employ SQP to design quincunx filter banks with PR, linear phase, high coding gain, good frequency selectivity, and certain prescribed vanishing moments properties. New quincunx filter banks designed using this SQP-based method were presented, and their effectiveness for image coding was demonstrated through experimental results. The SQP-based design technique was compared to our previously proposed SOCP-based method. The optimal solutions obtained by these two methods achieve comparable performance, while the SQP-based method generally requires fewer iterations to converge. Moreover, for small-sized design problems, the total execution time of the SQP-based method is usually less than that of the SOCP-based technique.

8. REFERENCES

[1] D. B. H. Tay and N. G. Kingsbury, "Flexible design of multidimensional perfect reconstruction FIR 2-band filters using tranformations of variables," *IEEE Trans. on Image Processing*, vol. 2, no. 4, pp. 466–480, Oct. 1993.

[2] W. Sweldens, "The lifting scheme: A custom-design construction of biorthogonal wavelets," *Applied and Computational Harmonic Analysis*, vol. 3, pp. 186–200, 1996.

[3] R. Fletcher, *Practical Methods of Optimization*, Wiley, New York, NY, USA, 2nd edition, 1987.

[4] A. Gouze, M. Antonini, and M. Barlaud, "Quincunx lifting scheme for lossy image compression," in *Proc. of IEEE International Conference on Image Processing*, Sept. 2000, vol. 1, pp. 665–668.

[5] J. Kovacevic and W. Sweldens, "Wavelet families of increasing order in arbitrary dimensions," *IEEE Trans. on Image Processing*, vol. 9, no. 3, pp. 480–496, Mar. 2000.

[6] Y. Chen, M. D. Adams, and W.-S. Lu, "Design of optimal quincunx filter banks for image coding," *EURASIP Journal on Advances in Signal Processing*, vol. 2007, pp. Article ID 83858, 18 pages, 2007, doi:10.1155/2007/83858.

[7] J. Katto and Y. Yasuda, "Performance evaluation of subband coding and optimization of its filter coefficients," in *Proc. of SPIE Visual Communications and Image Processing*, Nov. 1991, vol. 1605, pp. 95–106.

[8] J.F. Sturm, "Using SeDuMi 1.02, a MATLAB toolbox for optimization over symmetric cones," *Optimization Methods and Software*, vol. 11–12, pp. 625–653, 1999.